

Scratching Mechanisms of Hip Artificial Joints

Based on the results obtained from experimental and numerical previous studies, the authors try to evaluate the wear evolution in the components of a Total Hip Prosthesis (THP), during the service period. Topographic investigations of polyethylene cup and femoral head surfaces, of a modular total hip prosthesis, retrieved after 10 years service period, are made. The aim of this study is to identify the damaging mechanism of a 28 mm TiAl4V femoral head and his influence on the UHMWPE acetabular cup wear. For this purpose one analyses: the state of surfaces (roughness, micro hardness), surfaces wear type, localization and microscopic investigation of damages, wear mechanism identification.

Keywords: Total Hip Prostheses, embedded particle, wear

1. INTRODUCTION

Total Hip Prostheses are successfully solutions in Total Hip Arthroplasty (THA) surgery, having an estimate service period of about 15 years. Throughout the world, about 1000 THA are daily made and about 10% from them are Total Hip Replacements (THR).

The hip prosthesis stability is influenced by many factors and among them one mentions: scratching of the metallic femoral head by wear particles (bone, cement, or metallic debris) [1], wearing and deformation of the femoral head, osteolysis caused by ultra high molecular weight polyethylene (UHMWPE) and cement debris, synovial membrane congestion due to wear particles.

It is well known that there is a wide distribution of UHMWPE particles size in periprosthetic tissue. Particles smaller than 1 μm are the most active ones from a biological point of view [2], [3]. The scratches occurring on femoral head could be considered as main cause of increased intensity of wear rate [4]. Brown et al.[5] reported that modifications of femoral head roughness have a significant impact on UHMWPE wear.

It was noticed that there is a strong relation

*Lucian Căpitanu, Justin Onisoru, Aron Iarovici,
Constantin Tigăneșteanu
INSTITUTE OF SOLID MECHANICS, Romanian
Academy, 010141 Bucharest, ROMANIA*

between the scratching of femoral head and the presence of foreign third bodies (bone, cement or metallic particles), usually embedded in the acetabular cups and periprosthetic tissue [6]. Especially for modular prostheses and for those having porous coatings the quantities of worn particles are quite significant. Anyway, the wear mechanism due to head scratching is still controversial.

2. EXPERIMENTAL PROCEDURE

The experimental studies were performed on prosthetic components resulting from a THR revision.

The analyzed prosthesis has a cemented femoral component with modular head and the acetabular polyethylene liner, inserted in a metallic Harris Galante cup, having metallic coating.

Following visual inspections, some local rubbing and a severe scratch could be located on femoral head, caused probably by a hard particle embedded in the UHMWPE cup. The authors assume that the hard body causing the severe scratches could result from the damaging of the metallic coating of Harris-Galante cup.

For a more accurate picture of the femoral head surface deteriorations the procedure described by Najjar et al in [6] was adopted. Basically, by

intermediate of 5 parallels (from A to E in Figure 1) and 6 meridians (from 1 to 6 in Figure 1) the femoral head was divided in 36 regions.

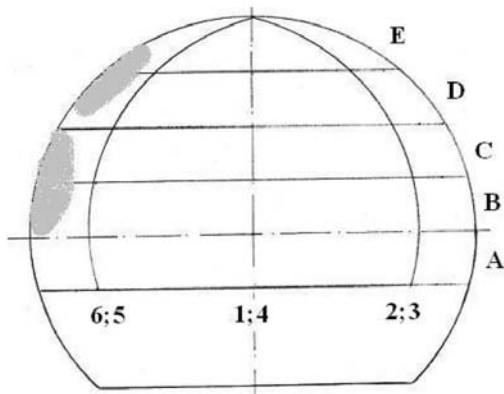


Fig. 1: Head regions inspected and scratching wear identified in 5D and 5C zone

The out-of-roundness deviation was measured on the B(equatorial), C(median) and E(upper) parallels. The results presented in Figure 2 show for upper parallel E significant deformations of femoral head with respect to its original shape considered perfectly spherical.

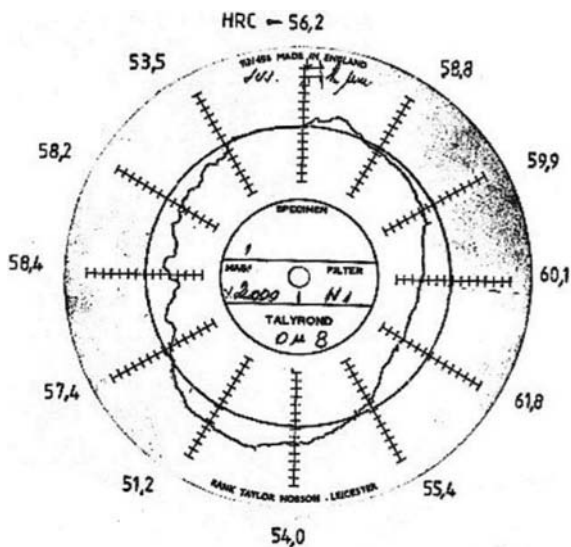
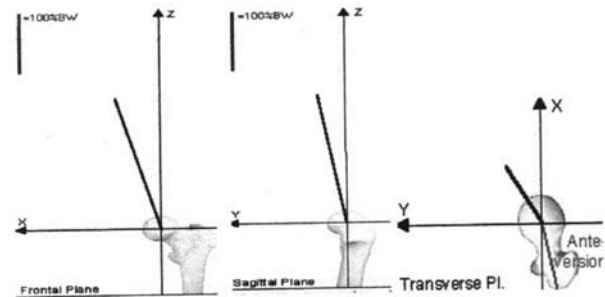


Fig. 2. Out-of-roundness of a femoral head, record on E parallel, for a revised Total Hip Prosthesis

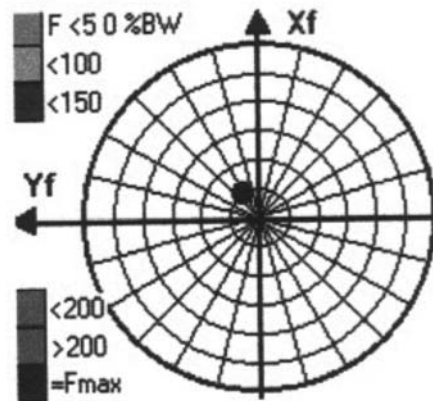
The arithmetic medium roughness R_a , that measure the medium absolute deviation of asperities heights from the reference line, was investigated together with the BT-042-2 femoral head surface hardness (micro hardness measurements) at the intersections between parallels and meridians using a ultrasonic hard meter (Figure 2).

Due to the variations of direction and magnitude of resultant force acting on the femoral head during walking cycle (telemetrically measured by Davy et al [9], the hip joint experiences a combined tension/compression and torsion loading regime.

Using previous experience, Bergmann et al. designed a telemetric prosthesis for measuring the magnitude and the direction of resultant force acting on hip artificial joint (see Figure 3, from [7]). The hip joint force is represented in anatomical coordinate planes (Fig.3a), and the locus of the appliance of it, on the femoral head, is revealed in Fig. 3b. One could see that the resultant angle in the frontal plane is 21.25° , independent of walking speed, but in the transverse plane the angle varies between 15 and 30° , based on the walking speed variation.



(a)



(b)

Fig. 3. The projections of the hip joint resultant force onto anatomical coordinates planes (a) and the locus of it on the femoral head (b) (from [7])

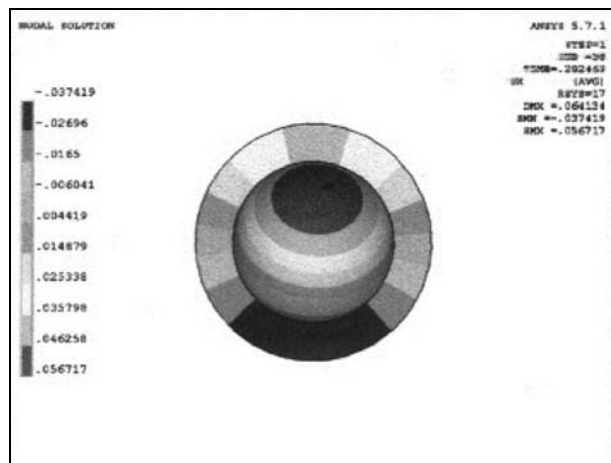
Based on the results reported in the contributions mentioned above, one could consider that the deformation of the femoral head is basically due to the compression on the resultant force direction. The authors use the results obtained by Bergmann et al [7] in order to obtain by Finite Element Method a more detailed image of the stresses and displacements distribution in the components of femoral head/acetabular cup couple [8].

The FE analysis, performed using ANSYS, considers that the transfer mechanism of the loading through the joint components is realized by intermediate of the elastic frictional contact, between the femoral head and the UHMWPE cup.

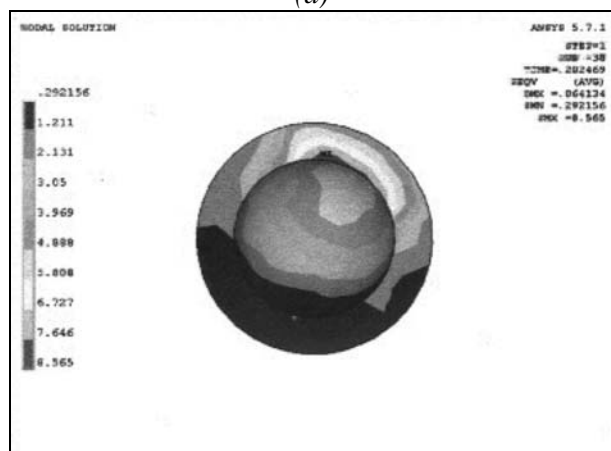
The loading sequence is obtained by dividing the resultant force diagram, reported in [7], in 200 load steps over 1.2 seconds of the walking active cycle.

3. EXPERIMENTAL RESULTS

Distribution of radial displacements and von Mises stresses in the UHMWPE cup, corresponding the 38 interval of loading, where the maximum resultant force are obtained, are presented in Figures 4a and 4b. Examining the plots presented in Figures 4a and 4b, one could notice not only the maximum magnitude of the measured parameters (radial displacements . 0.0567 mm, and von Mises stresses . 8.62 MPa) but also the direction of the resultant force acting on the joint - revealed by the contact spot.



(a)



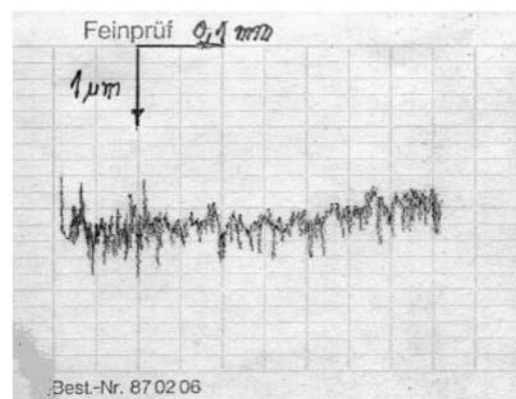
(b)

Fig. 4. Maximum radial displacements (a) and von Mises stresses (b) in UHMWPE acetabular cup

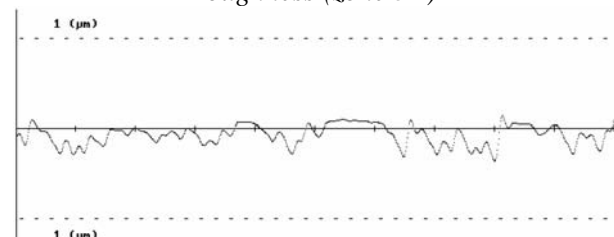
By out-of-roundness checks, some ovalizations of femoral head are revealed . over 180 μm on parallel E , presented in Figure 2, 164 μm on parallel C and approximately 78 μm on equatorial parallel. Micro hardness measurements indicate also some local hardening of the compressed areas.

Investigation of surface roughness, R_a gave us median indications regarding the variation of asperities height from one point to other, with no information related to the spatial distribution or topographical pattern. The roughness plots, made for three of the 36 delimited areas of the femoral head, are presented in Figure 5a, 6a and 7a.

These plots, obtained by using a contact profilometer (Perth-O-Meter) with needle radius of 2,5 μm and compressive force of 20 mN, are acquired and processed in order to determinate some estimates of the topography of the investigated area .



a) Graphic representation of the processed trace roughness (zone 5E)



b) Zone: 5E. Computation of the graphic representation of the trace roughness. Total number of samples: 1001. Specimen length (mm): 0.125125



c) Zone: 5E. Height distribution. Interval length: 0.06(μm /interval)



d) Zone: 5E. Abbott Firststone curve of the surface.
Interval length: 0.06 ($\mu\text{m}/\text{interval}$)

182	2576
3525	2329
3631	2326
5377	2323
395	2315
7541	1281
164	1306
9857	1309
4149	1326
368	1473

Rt = 1.158318 (μm)
Rz = .9255814

Ra, rms, sqw = 9.890832E-02 .1298455 .113496

e) Computation of : Rt, Rz, Ra, rms, sqw

Fig. 5. Computation of statistic data obtained by investigating the topography of 5E region



d) Zone: 6B. Abbott Firststone curve of the surface.
Interval length: 0.06 ($\mu\text{m}/\text{interval}$)

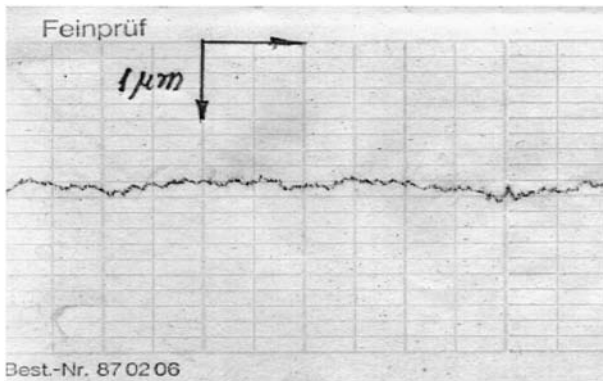
6060	2232
633	2226
2572	2221
5120	2208
5103	2204
9664	1553
9733	1621
7580	1789
2121	1816
2388	1852

Rt = .6073346 (μm)
Rz = .4400716

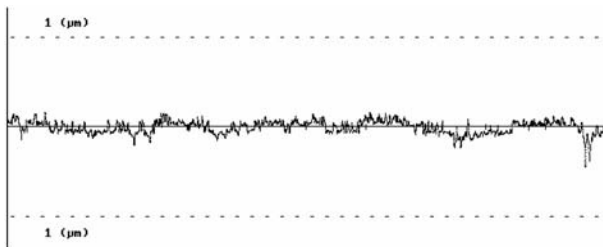
Ra, rms, sqw = 5.712492E-02 6.976814E-02
-.8561983

e) Computation of : Rt, Rz, Ra, rms, sqw

Fig.6. Computation of statistic data obtained by investigating the topography of 6C region



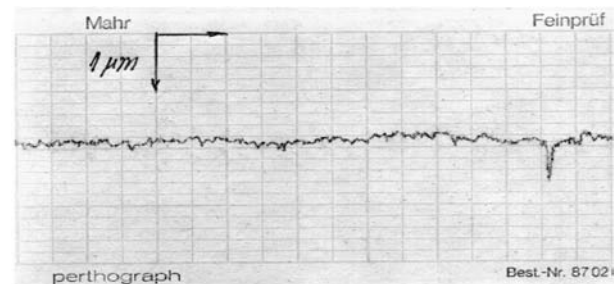
a) Graphic representation of the processed trace roughness (zone 6C)



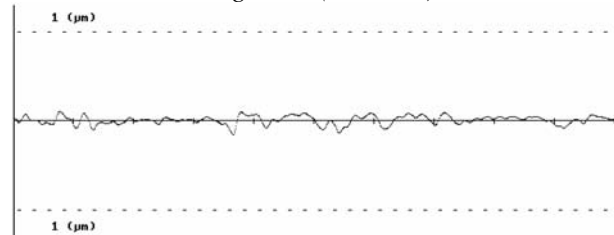
b) Zone: 6C. Computation of the graphic representation of the trace roughness. Total number of samples: 1001. Specimen length (mm): 0.125125



c) Zone: 6C. Height distribution. Interval length: 0.06 ($\mu\text{m}/\text{interval}$)



a) Graphic representation of the processed trace roughness (zone 3D)



b) Zone: 3D. Computation of the graphic representation of the trace roughness. Total number of samples: 1001. Specimen length (mm): 0.125125



c) Zone: 3D. Height distribution. Interval length: 0.06 ($\mu\text{m}/\text{interval}$)



d) Zone: 3D. Abbott . Firststone curve of the surface. Interval length: 0.06 ($\mu\text{m}/\text{interval}$)

9480	2245
9673	2230
9641	2211
8997	2210
602	2209
640	1672
32	1742
7305	1761
5277	1795
7210	1798

Rt = .5125223 (μm)
Rz = .418068

Ra, rms, sqw = 5.054321E-02 6.413104E-02
-9.304123E-02

e) Computation of : Rt, Rz, Ra, rms, sqw

Fig. 7. Computation of statistic data obtained by investigating the topography of 3D region

By intermediate of the two conditions above, the median line could be determined, but the process of graphical evaluation . based on the effective profile . is a difficult one. The electronic integrative circuits of the needle profilometers evaluate generically a line that is parallel with the macrogeometrical profile and for which the sum of areas delimited by the real profile below and above this line, are equals. This line which differs from the median line for a general profile is called central line. For a periodic profile the two lines are coincidental.

Based on the median line and surface profile, some characteristic measures could be evaluated as follows. The median deviation of profile R_a , is defined as the median value of the ordinates of profile points versus the median line (see eq.1):

$$R_a = \frac{1}{l} \int_0^l |y| dx \quad (1)$$

or approximately:

$$R_a = \frac{\sum_{i=1}^{i=n} |y_i|}{n} \quad (2)$$

The asperities height, R_z , is defined as being the difference between the average ordinate of highest and lowest five points of the profile. These ordinates are measured inside the limits of the basis length, based on a parallel to the median line, located outside the outer and inner lines:

$$R_z = \frac{1}{5} \sum_{i=1}^{i=5} R_i - \frac{1}{5} \sum_{j=1}^{j=1} R_j \quad (3)$$

where R_z , basically a measure of the height of the surface asperities, is estimated based on visual and tactile inspections of the surface. This parameter is strongly influenced by the presence of scratches and micro-cracks.

The maximum height is defined as the distance between the exterior and interior lines. The height distribution is presented in Figure 5c, 6c and 7c.

When a surface undulation occurs, the measures R_a and R_z are strongly influenced by the value of basis length of investigated interval, l . The electronic circuit of needle profilometer, allow for choosing the basis length reducing the effect of undulations. In addition to R_a , R_z and R_{max} , the M-system based on the median line of the profile allow for determination of other values as:

- standard deviation rms or σ , defined by:

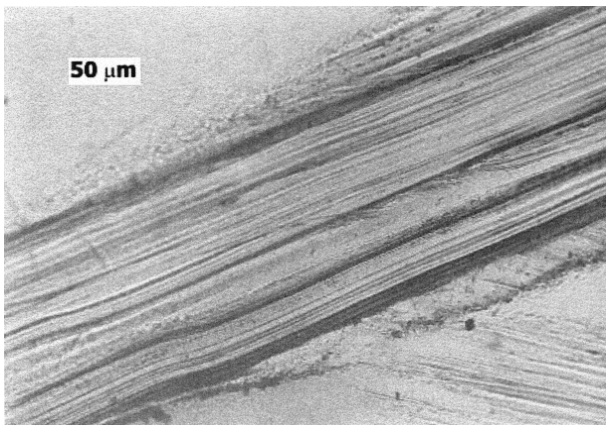
$$\sigma = \sqrt{\frac{1}{l} \int_0^l y^2 dx} \quad (4)$$

- the bearing length L , defined by equation :

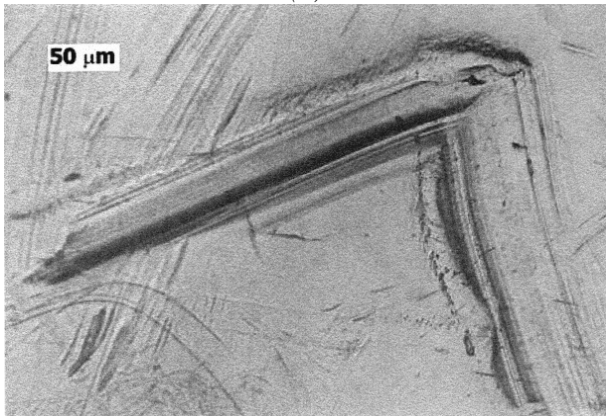
$$L = \sum l_p \quad (5)$$

The bearing length, defined in relation with asperities height, determine the bearing lift curve Abbott . Firststone, see Figure 5d, 6d and 7d . which could be used in order to evaluate the wear and the polished surface. This reveals the behavior of surface microgeometry during the external loading. Basically, the Abbott . Firststone curve could be used for computation of the material quantity that need to be given away in order to obtain a bearing surface. The mean depth, defined as difference between the median line and the inner one, and the filling factor defined as the ratio between the median depth and R , could be computed also.

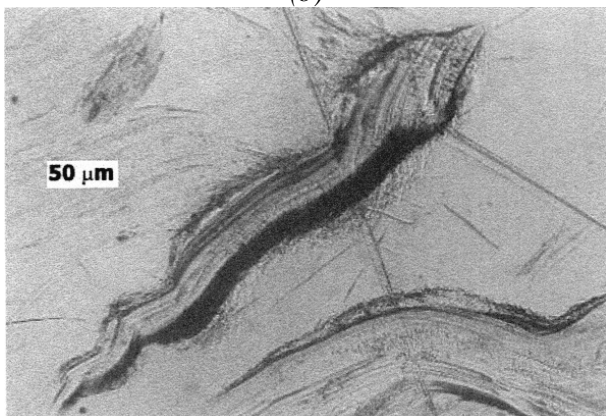
For an arbitrary chosen profile, there is no correlation between the measures defined above. It is considered that the ratio R_{max}/R_a is somewhere around 3.5.



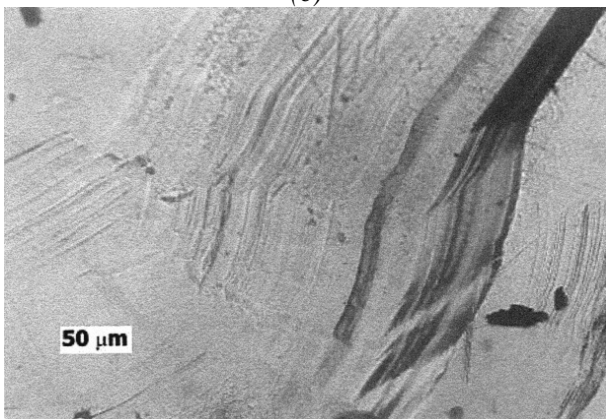
(a)



(b)

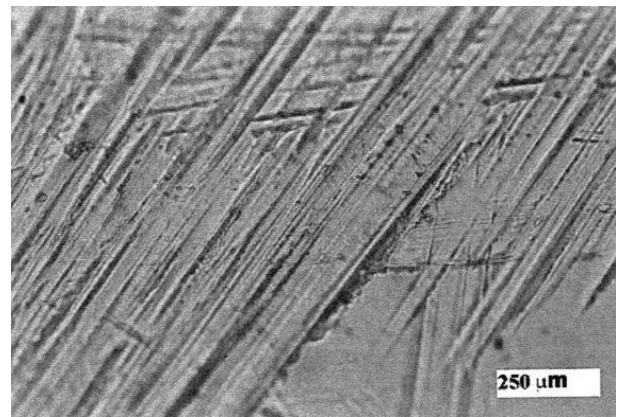


(c)

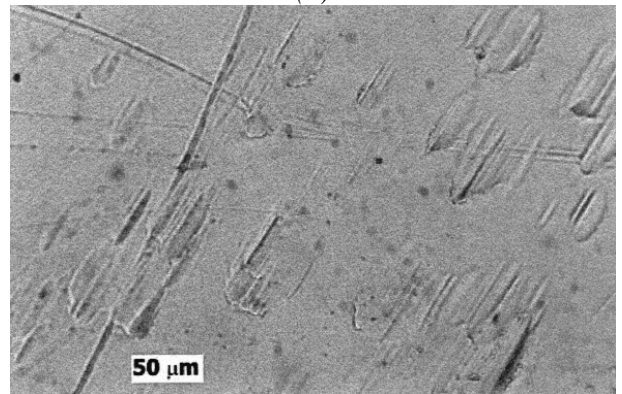


(d)

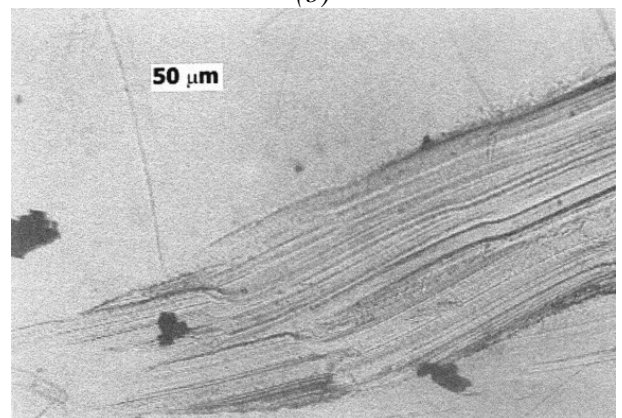
Fig. 8. Scratching of femoral head in 5E zone (a, b, c and d)



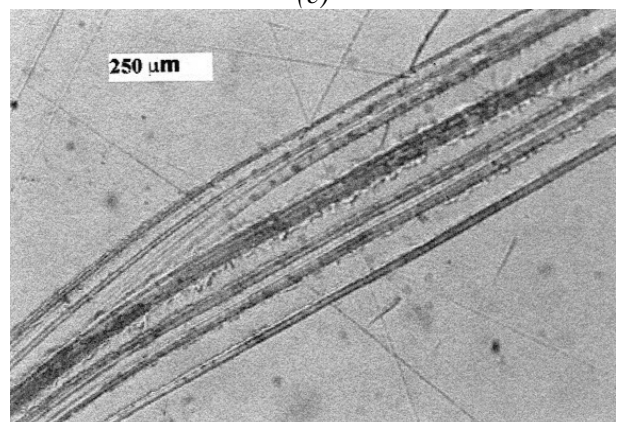
(a)



(b)

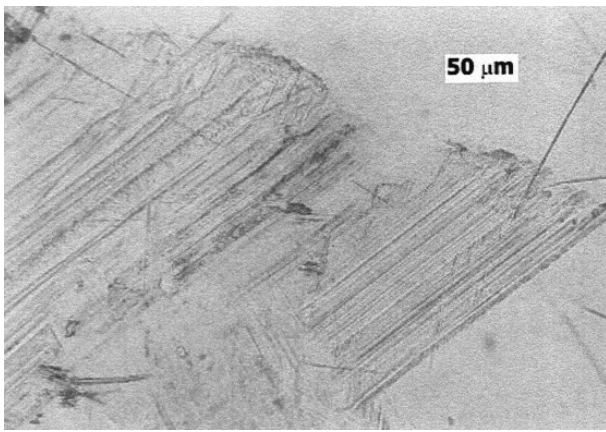


(c)

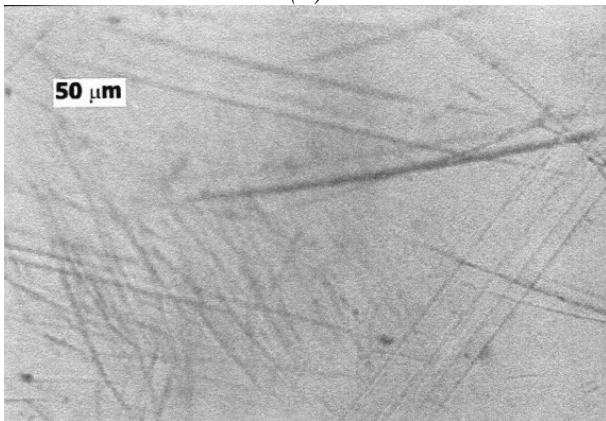


(d)

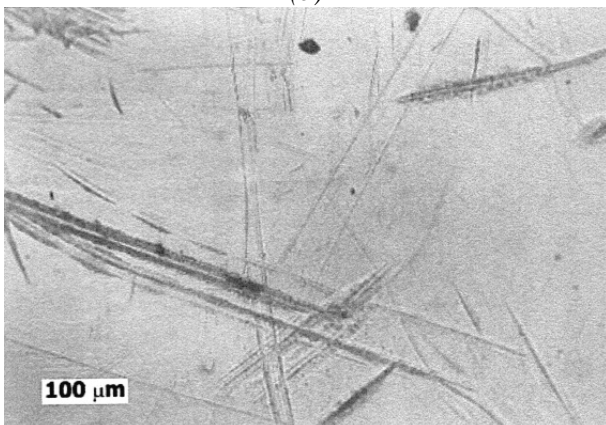
Fig. 9. Scratching of femoral head (a, c and d) and local plastic deformations (b) in 5C zone



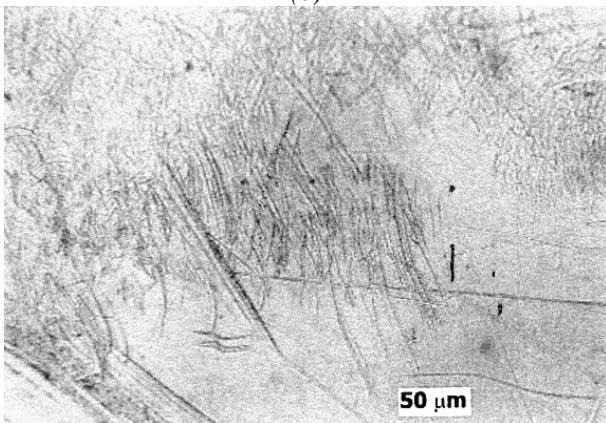
(a)



(b)

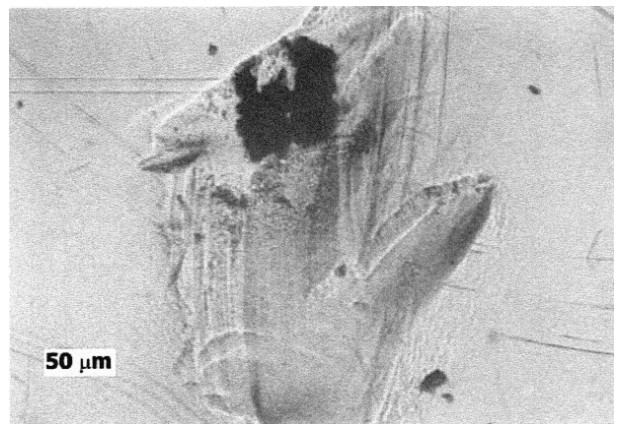


(c)

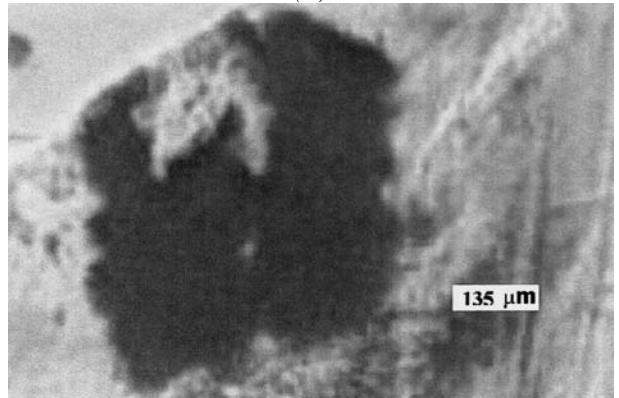


(d)

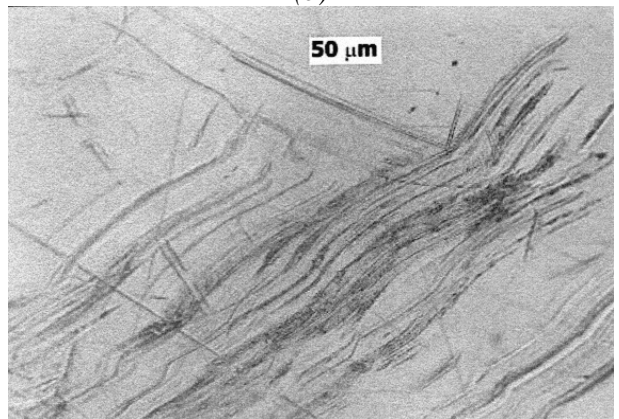
Fig.10. Polishing (a, b and d) and scratching (c) of femoral head in 5E zone



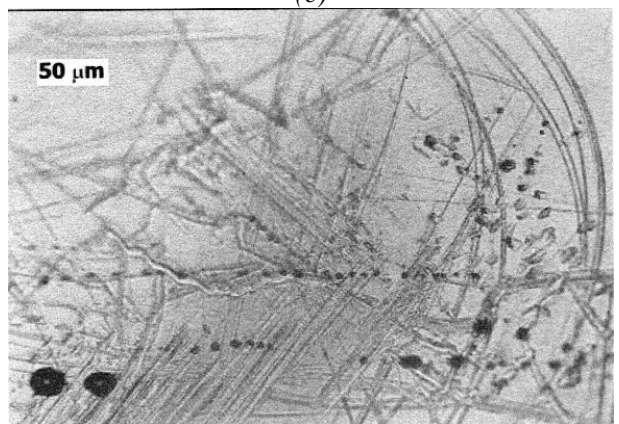
(a)



(b)

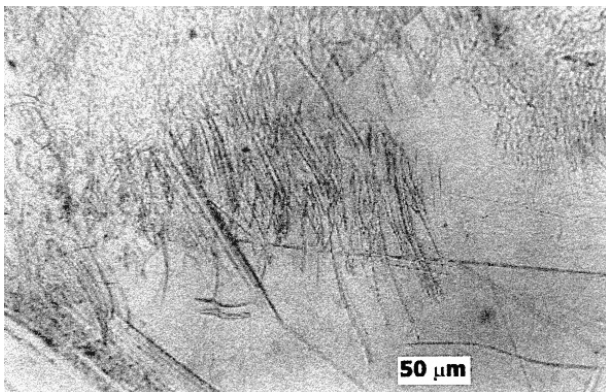


(c)

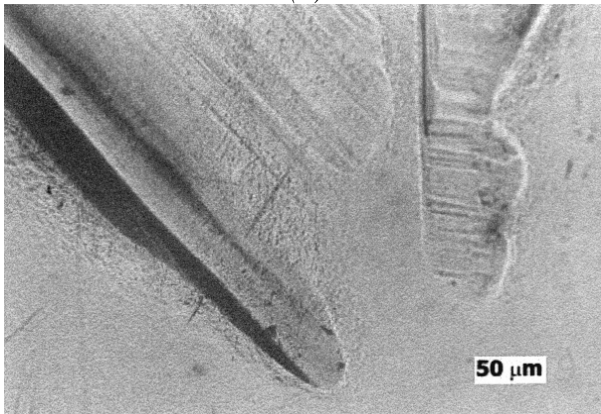


(d)

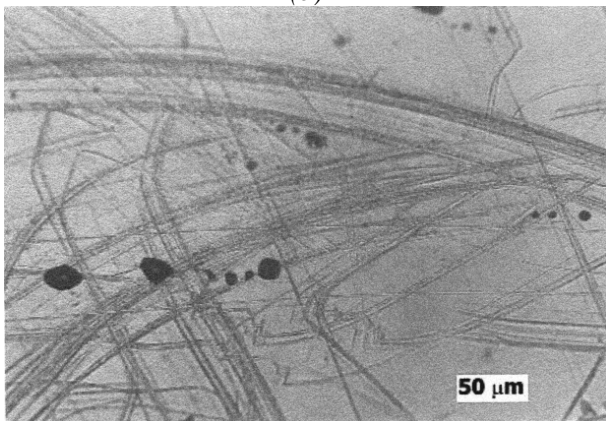
Fig.11. Scratching (c), embedded wear particle (a and magnified image in b) and corrosion fretting (d) of femoral head in 6B zone



(a)



(b)



(c)

Fig.12. Polishing of femoral head surface in 5F zone, scratching in 2D zone (lower area) and corrosion fretting in 1D zone

The optical microscopy study, of the 36 regions delimited on the femoral head, revealed that 25% of the entire surface has isolated micro-scratches despite of polished macroscopic aspect. More than that, in the area of intersections between 5 and 2 meridians with E, D and C parallels, some seriously damaged regions are identified covering 15-20% of the femoral head surface.

The more severe wear is observed in region 5E, located between 15 and 30° in transversal plane (see Figure 10 . a, b, c, and d), around the locus of

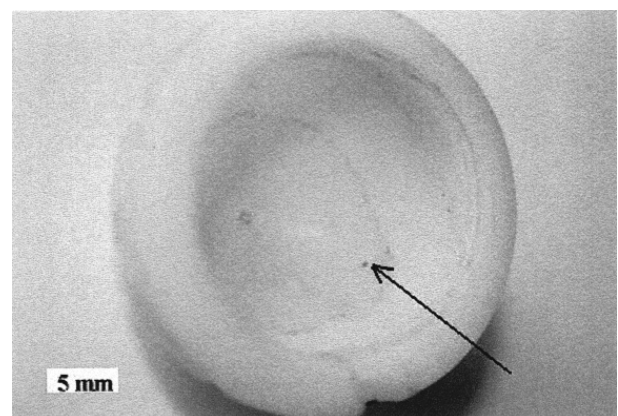
the point where the resultant force intersect the sphere of femoral head . as identified by Bergmann et al in [7].

The large scratch could be related to the abrasion due to third body, namely the wear particles. Local yielding of some restraint areas on the femoral head surface was revealed especially in regions 5E (Figure 8 a,b, c and d) and 5C (Figure 9 a, b, c and d). A closer look to the region 6B identified an embedded wear particle which scratched the femoral head surface (see Figure 11a and b). Signs of severe micro cutting were detected also in region 6B and 2D- lower area (see Figure 11c and 12b).

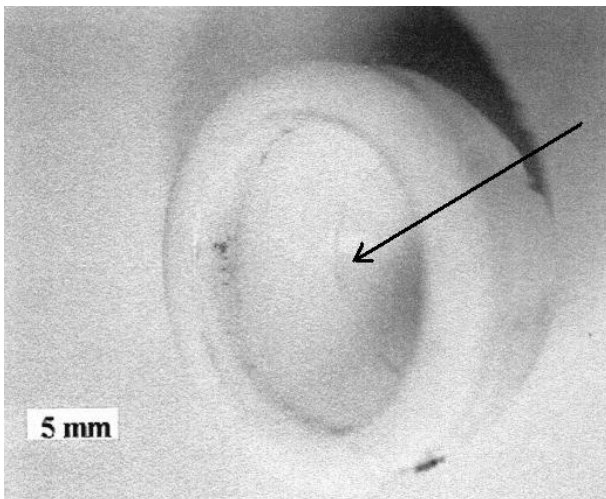
In Figure 9b, one could observe some local plastic deformations of the 5C region (b), scratching of femoral head (a, c and d). In Figure 11d and 12c one could observe small scratches and pits produced by biotribological corrosion.

The corrosion pits occurred due to strong mechanical loading combined with the local temperature increase, at the contact interface. This is the corrosion fretting wear effect. Generally, the fretting is considered as surfaces damage, of two bodies in contact, due to an oscillatory slipping of relative small magnitude. This oscillatory movement may be the result of contact bodies. deformation, due to variable traction, torsion or bending. This surface damage implies the fretting wear and the fretting fatigue.

The main source of surface damages of the UHMWPE acetabular cup is represented by the wear particles embedded in the exterior layer of femoral head. Depending on the geometry and provenience of the embedded particle, abrasive rifles could occur following the relative motion of the joint active elements.



(a)



(b)

Fig.13. Picture of UHMWPE acetabular cup: fretting wear (a) and embedded wear particle (b)

A metallic wear embedded particle has been identified inside the UHMWPE acetabular cup (see Figure 13a). The acetabular cup surface damages, by fretting wear, is presented in Figure 13b.

4. CONCLUSIONS

The identified roundness deviations of the femoral head (180 μm on parallel E, 164 μm on parallel C and 78 μm on equator) are quite large exceeding the value of 0.05 μm , which is identified in ISO 7206-2 as being the limit for median roughness of the metallic surface of a hip prosthesis femoral head.

Also, the micro hardness differences between the compressed and non-compressed areas are actually large (approximately 9 HRC). It results that the biotribological system represented by the femoral head/acetabular cup couple is modifying on the long term two of its input parameter, namely the geometrical shape and the local hardness of the metallic surface of the femoral head.

For the investigated femoral head, the following maximum values of roughness estimates are obtained (in region 5C . see Figure 7e): $R_a = 0.09 \mu\text{m}$, $R_t = 1.158318 \mu\text{m}$, $R_z = 0.9255814 \mu\text{m}$, $rms = 0.1298455$ respectively $sqw = -1.13496$. Those values stand for a two times exceedance of ISO 7206-2 allowable limits for femoral head surface.

The roughness of femoral head active surface has a regional non-uniform increasing during the service period, which contributes to the increased wear of

the UHMWPE acetabular cup. As a general assertion, one could consider that abrasive wear particles occurred at the active contact interface of a hip prosthesis, could lead to the damaging of the femoral head surface by scratching it and subsequently could accelerate the wear of the femoral head/acetabular cup biotribological system.

Acknowledgements

The authors wish to express their gratitude to Romanian Academy and the Research and Educational Ministry (MEC) for its support of the program of work reported herein. The work took place as part of the research projects no. 120/2004-2006 and 127/2005-2007 in the framework of Grants of CNCSIS (Romanian National Council for Scientific Research).

REFERENCES

- [1] Najjar D, Bigerelle M, Migaud H, Iost A. *Identification of scratch mechanisms on a retrieved metallic femoral head* ., Wear 258 (2005),240-250.
- [2] McNie, C.M., Barton, D.C., Ingham, E., Tipper, J.L., Fischer, J., Stone, M.H. *Modelling of damage to articulating surfaces by third body particles in total joint replacements*., J.Mater.Sci.Mater.Med. 11(2000), 569-578.
- [3] Tipper, J.L., Ingham, E., Hailey, J.L., Besong, A.A., Fischer, J., Wroblewski, B.M., Stone, M.H., *Quantitative analysis of polyethylene wear debris, wear rate and head damage in retrieved Charnley hip prostheses*., J.Mater.Sci.Mater.Med., 11(2000), 117-124.
- [4] Elfick A.P.D., Smith S.L., Green S.M., Unsworth A., *The quantitative assessment of UHMWPE wear debris produced in hip simulator testing; the influence of head material and roughness, motion and loading* ., Wear 249 (2001), 517-527
- [5] Brown T.D., Stewart K.J., Nieman J.C., Pedersen D.R., Callaghan., *Local head roughening as a factor contributing to variability of total hip wear; a finite element analysis*., J.Biomech. Eng.124 (2002),691- 698
- [6] Najjar D., Behnamghader A., Iost A., Migaud H., *Influence of a foreign body on the wear of metallic femoral heads and polyethylene acetabular cups of total hip prostheses*. J.Mater.Sci.Mater.Med.35(2000), 4583-4588

[7] Bergmann G, Deuretzbacher G et.al., . *Hip contact force and gait patterns from routine activities* . J. Biomech. Eng.,34 (2001), 859-871

[8] Capitanu L. .The orthopaedical endoprotheses durability., BREN , Bucharest, 2004 (in Romanian)